DINAME 2023 - Proceedings of the XIX International Symposium on Dynamic Problems of Mechanics,
A.S. De Paula, A.T. Fabro and M.R. Machado (Editors), ABCM.
Pirenópolis, Go, Brazil, February 26th to March 3rd, 2023

Standing Self-Balancing Wheelchair

Renan Imamura Marques [1] and Décio Crisol Donha [2]

[1, 2] University of São Paulo, Polytechnic Scholl

Abstract: This paper describes the design and build of a small-scale prototype of a personal transporter for users with physical disabilities. The transporter allows the user to move similarly to a person without physical disabilities in an upright and balanced position and it is intended to work both as a regular electric wheelchair on four points on the ground or in an upright and balanced position supported by two parallel wheels on the ground, like a Segway. The paper presents the dynamic modeling of the system and the design of the multivariable controller by pole placement. The experimental work involves the use of an Arduino Mega control board, programmed in the C language, sensors, and the hardware to drive the two DC motors. The controller stabilize the wheelchair in the upright position, rejecting disturbances such as gentle pushing. The paper presents analytical and experimental results.

Keywords: personal transporter, upright position, balanced position, Segway, Arduino Mega.

INTRODUCTION

Currently, there are automated electric wheelchairs capable of providing greater comfort and mobility to people with reduced mobility. Robotic systems and advanced automation applied to personal transporters enable physically disabled users to move similarly to normal persons. Thai, Tai and Tien (2020), for example, designed and implemented a flexible electric wheelchair capable of changing the position of the seat according to the user's demand. The wheelchair is also able to change its mechanical structure to operate on different terrains. At the Wuhan University of Technology, Deng, Dong, and Chen (2021) developed a chair based on parallel bar mechanisms that allows the user to climb and descend stairs and safely overcome obstacles. Jameel, Mohammed and Gharghan (2020) employed a strategy to control a motorized wheelchair based on gyroscopic signals installed on a device used on the user's head. The solution, aimed at quadriplegics, allows the wheelchair to be controlled by the movement of the user's head. There are commercial technological solutions for increased mobility and comfort for people with disabilities. As an example, *Freedom Stand up* allows the user to stay statically in the upright position. Also noteworthy is the *S-Pod* wheelchair, developed by *Segway*. It is an adaptation of a conventional *Segway* but in the form of a wheelchair. Like the *Segway*, the *S-Pod* wheelchair is a self-balancing device that rests on the floor using two parallel wheels. The product however does not allow the upright position. This work presents the development of a small-scale prototype of a wheelchair that allows the locomotion of a disabled person in an upright and balanced position using some of the solutions mentioned above.

Many control strategies are applied to self-balanced systems based on two parallel wheels. As it is an unstable and non-linear system, it is ideal for the application of control techniques in addition to being a system of great relevance and applicability. Su et al. (2020) used a nonlinear adaptive control system to improve the stabilization of a self-balanced robot on two wheels. They verified through experiments that the non-linear adaptive controller presented a better performance than linear PID controllers. Fahmi et al. (2020) proposed the use of optimal control for the stabilization of a self-balanced wheelchair, reporting excellent performance. The mathematical model used to synthesize the control law in this work was based on the research developed by Mohammed, and Abdulla (2020), in which they performed the control of a *Segway* using an LQR controller.

For future work, it is intended to develop a controller design using robust control techniques as in Kien, Quang and Trung (2021) and Kin and Park (2016). This is to ensure that the wheelchair works properly with different users, considering parameters such as its height and weight, guaranteeing greater safety.

This paper is as follows. The sections 2 and 3 describe the development of the system model and the system analysis respectively. Section 4 describes the controller development. Section 5 shows the hardware architecture. The practical results are presented in section 6. Finally, section 7 brings the conclusions.

SYSTEM MODEL

The prototype is intended to be constructed in aluminum and wood. The mechanism responsible for the switching of the structure between the sitting and the standing positions is composed of a parallel bar mechanism. The CAD model and the final small-scale prototype can be seen in Fig. 1 and Fig. 2, respectively, as shown below.

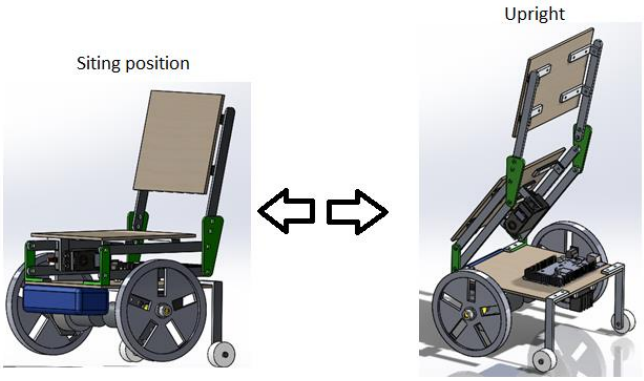

Figure 1 – CAD model of the prototype.

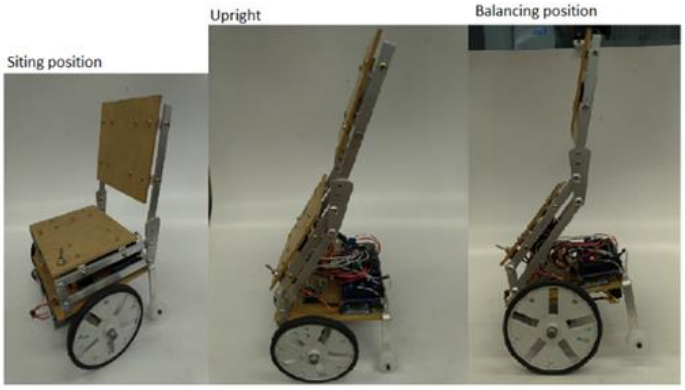

Figure 2 – Sitting, upright, and balancing wheelchair position.

The control system is only active when the wheelchair is in the upright position and when the chair is balanced on only two wheels. Therefore, the mathematical model described in this section represents the wheelchair only in this condition.

System elements

The system has four states, position and speed of the wheels, angular position and angular speed of the wheelchair. Of the four states of the system, two are outputs, that is, variables to be controlled, wheel position and angular position of the wheelchair. The system has only one input, the electromotive voltage applied to DC motors.

To develop the wheelchair controller, it was considered disturbances caused by forces applied to it, such as small pushes or collisions with objects in the environment.

The following hypotheses were adopted to simplify the mathematical model of the system. The speed of the DC motor is assumed proportional to the electromotive force applied to its terminals. The torque of the DC motor is assumed proportional to the current. The mechanical system is slow compared to the electrical system and in this way allows current transients to be omitted. It was assumed that there was no slip between the wheels and the ground. The forces exerted by the wheels are considered equal, and therefore just doubled in the mathematical model. The difference in speed between the two wheels is considered insignificant. The centripetal force of the pendulum is considered small and therefore omitted. Since the system is non-linear, the model will be linearized at the equilibrium point, when the wheelchair is in the upright position. To simulate a more realistic case, an error is introduced in the angular position other than the equilibrium position.

The next sections describe the electrical and mechanical wheelchair model development.

Electrical System

The wheelchair DC motors were modelled as controlled by the current of the armature using the circuit below, where R and L represent the resistance and inductance of the motor, and U, U_e and i represent input voltage at the motor terminals, the electromotive force and the electric current, respectively.

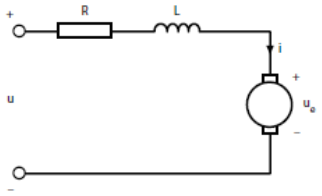

Figure 3 – Direct current electric circuit.

The electromotive force is assumed, as usual, to be proportional to the angular velocity through the velocity constant K_e, as follows:

$$U_e = K_e(\dot{\theta_w} - \dot{\theta_b})$$

Where θ_w and θ_b represent the wheel and wheelchair angular velocity, respectively.

The T_1 torque produced by the DC motor is assumed to be proportional to the current i through the torque constant K_m as follows:

$$T_1 = K_m.i \tag{1}$$

Using Kirchhoff´s law, the electrical circuit model is then given by:

$$U = R.i + L.\frac{di}{dt} + U_e \tag{2}$$

Mechanical System

The mechanical system is divided into two subsystems, the wheels, and the wheelchair body. These subsystems free body diagrams are respectively shown in Fig. 4 and Fig. 5 below.

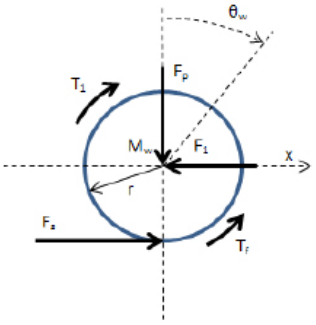

Figure 4 – Wheels free body diagram.

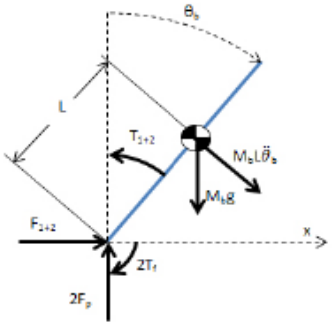

Figure 5 – Wheelchair (upright position) free body diagram.

Since we assumed that the mechanical system is slow compared to the electrical system, the current transient is omitted and the derivative term in Eq. (2) is considered null. Isolating the current variable in Eq. (2) gives:

$$i = \frac{U - U_e}{R} = \frac{U}{R} - \frac{K_e}{R}.(\dot{\theta_w} - \dot{\theta_b})$$

Substituting the above expression into Equation 1, the expression of torque is obtained as follows:

$$T_1 = \frac{K_m}{R}.U - \frac{K_e.K_m}{R}.(\dot{\theta_w} - \dot{\theta_b}) \tag{3}$$

The equations of motion of the wheels are then given by:

$$J_w.\ddot{\theta}_w = T1 - r.F_s - T_f \tag{4a}$$

$$M_w.\ddot{X}_x = F_s - F_1 \tag{4b}$$

Where J_w is the wheel inertia, F_s is contact force between the wheels and surface, T_f is the friction torque and r is the wheels radius.

It is assumed that there is no slip between the wheels and the surface, therefore, the wheel acceleration can be expressed as:

$$\ddot{X}_w = \ddot{\theta}_w.r$$

The equation of motion for the wheelchair body in the horizontal direction is as follows:

$$M_b.\ddot{X}_b = (F_1 + F_2) - M_b.L.\ddot{\theta}_b.\cos\theta_b \tag{6}$$

Where M_b is the wheelchair mass and $\ddot{X}_b$ is the horizontal wheelchair acceleration.

The last term is tangential to the horizontal component of the force. Index *1* in Eq. (6) represents the right wheel and index *2* represents the left wheel. The equation of motion referenced to the wheelchair center of mass is given by:

$$J_b.\ddot{\theta}_b = -(F_1+F_2).L.\cos\theta_b - (T_1+T_2) + 2.F_p.L.\sin\theta_b + 2.T_f \tag{7}$$

Where the J_b is the wheelchair body inertia.

The equation of motion for the wheelchair is as follows:

$$M_b.\ddot{X}_b.\cos\theta_b = (F_1+F_2).\cos\theta_b - M_b.L.\ddot{\theta}_b - 2.F_p.\sin\theta_b + M_b.g.\sin\theta \tag{8}$$

The F_p term represent de force between the wheelchair body and the wheels axis and g is the gravitational acceleration.

The wheels and the wheelchair body system model are obtained when the unknown expression of reaction of forces ($F_1 + F_2$) of Eq. (6), Eq. (5), and Eq. (4b) is found. It is assumed that any difference in speed between the two wheels is negligible.

$$M_b.\ddot{X}_b + M_b.L.\ddot{\theta}_b.\cos\theta_b = -2(M_w + \frac{J_w}{r^2}).\ddot{X}_w - \frac{2.K_e.K_m}{r^2.R}.\dot{X}_w + \frac{2.K_e.K_m}{r.R}.\dot{\theta}_b + \frac{2.K_m}{r.R}.U - \frac{2.T_f}{r}$$

Where M_w id the wheel mass. $\dot{X}_w$ and $\ddot{X}_w$ represent the horizontal wheels velocity and acceleration, respectively.

Introducing Eq. (7) into Eq. (8), a translation equation for the wheelchair body in terms of its rotation is obtained as follows:

$$(J_b + M_b.L^2).\ddot{\theta}_b = M_b.g.L.\sin\theta - M_b.\ddot{X}_b.L.\cos\theta_b + 2T_f - (T_1 + T_2))$$

where T_1 and T_2 are given by Eq.(3) and by the following model:

$$T_f = b.(\dot{\theta} - \frac{\dot{X}}{r})$$

Where *b* is the friccion viscous constant.

Note that this simplification omits the wheelchair body centripetal force, which was considered negligible.

The system is linearized and represented in the state space, assuming that the position x and the angular position θ are perfectly measured:

$$\dot{X} = A.x + B.u$$
$$Y = C.x + D.u$$

where *A* is a dynamic matrix, *B* is the input matrix, *C* is the output matrix and *D* is the direct input matrix.

In this application, *A* and *B* are given by:

$$A = \begin{bmatrix} 0 & 1 & 0 & 0 \\ 0 & \alpha & \beta & -r\alpha \\ 0 & 0 & 0 & 1 \\ 0 & \gamma & \delta & -r\gamma \end{bmatrix}$$
$$B = \begin{bmatrix} 0 & \alpha\varepsilon & 0 & \gamma\varepsilon \end{bmatrix}^T$$

Where:

$$\alpha = \frac{2(R_b - K_e K_m)(M_b L^2 + M_b r L + J_b)}{R(2(J_b J_w + J_w L^2 M_b + J_b M_w r^2 + L^2 M_b M_w r^2) + J_b M_b r^2)}$$
$$\beta = \frac{-L^2 M_b^2 g r^2}{J_b(2J_w + M_b r^2 + 2M_w r^2) + 2J_w L^2 M_b + 2L^2 M_b M_w r^2}$$

$$\gamma = \frac{-2(Rb - K_e K_m)(2J_w + M_b r^2 + 2M_w r^2 + LM_b r)}{Rr(2(J_b J_w + J_w L^2 M_b + J_b M_w r^2 + L^2 M_b M_w r^2) + J_b M_b r^2)}$$

$$\delta = \frac{LM_b g(2J_w + M_b r^2 + 2M_w r^2)}{2J_b J_w + 2J_w L^2 M_b + J_b M_b r^2 + 2J_b M_w r^2 + 2L^2 M_b M_w r^2}$$

$$\varepsilon = \frac{K_m r}{Rb - K_e K_m}$$

Table 1 gives the parameters of the system, which produced the state matrices presented before.

Table 1 - System parameters

Parameters	Value	Description
M_b	1.012 Kg	Mass
M_w	0.049 Kg	Mass of wheels
J_b	0.0067 Kg.m²	Moment of inertia to the CM
r	0.05 m	Radius of the wheels
J_w	5.02e-05 kg.m²	Moment of inertia of wheels
L_m	0.0369 m	Distance between axis and CM
K_e	0.5093 V.s/rad	Motor angular speed constant
k_m	0.2452 N.m/A	Motor torque constant
R	15.8 Ohm	Electric motor resistance
b	0.002 N.m.s/rad	Viscosity coefficient
g	9.81 m/s²	Gravitational acceleration

SYSTEM ANALYSIS

The system analysis is initially carried out by verifying the stability of the open loop system through its poles. Next, the controllability test is performed to verify if the system is controllable.

The system poles or the eigenvalues of the dynamic matrix *A* are as follows:

$$Poles = \begin{bmatrix} 0 \\ -11.75 \\ 6.04 \\ -3.09 \end{bmatrix}$$

As the system has a pole with a positive real part, it is unstable. The controllability was tested through the *ctrb Matlab* function, confirming the system controllability. It is interesting to point out that the instability of the system was already expected, as the wheelchair in the vertical position works like an inverted pendulum that is not in balance without a control system acting. Instability can also be verified through numerical simulations in the time domain, which is not presented for reasons of brevity.

CONTROLLER DESIGN

A control system is used to stabilize and guarantee good performance for the system. To carry out the controller design the pole placement was used. The poles for the system stability and the settlement time were chosen to achieve the desired performance. The poles were chosen according to the Bessel standard response, presented in Fig. 6 as are follows:

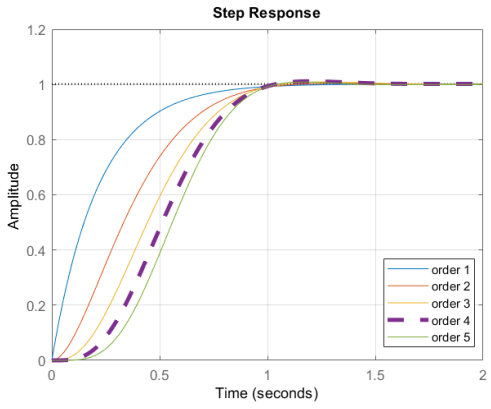

Figure 6 – Bessel standard response for 1 second setting time.

The data shown in Fig. 6 and table 2 were obtained through the *Matlab Bessel functions*.

Table 2 - Equation Poles for 1 second settling time

System Order	roots
1	-4.6200
2	-4.0530 ± 2.3400i
3	-5.0093, -3.9668 ± 3.7845i
4	-4.0156 ± 5.0723i, -5.5281 ± 1.6553i
5	-6.4480, -4.1104 ± 6.3142i, 5.9268 ± 3.0183i

Table 2 shows the poles for a 1 second settling time for different order systems. To avoid sudden reactions caused by the control system actuation, settling times of 1.4 seconds were chosen. Thus, the desired poles for the system were chosen as:

$$Desired\ poles = \begin{bmatrix} -2.86 + 3.62i \\ -2.865 - 3.62i \\ -3.94 + 1.18i \\ -3.94 - 1.18i \end{bmatrix}$$

The *Matlab place* function was used to determine the following controller gains:

$$K = \begin{bmatrix} -10.36 & -17.75 & -15.21 & -2.09 \end{bmatrix}$$

The simulation of the system in a closed loop was performed using *Simulink Matlab*. The system was simulated for a 0.15 rad error in the angular position of the wheelchair as a starting point. Fig. 7 illustrates the simulated voltage input to the motors and the output responses.

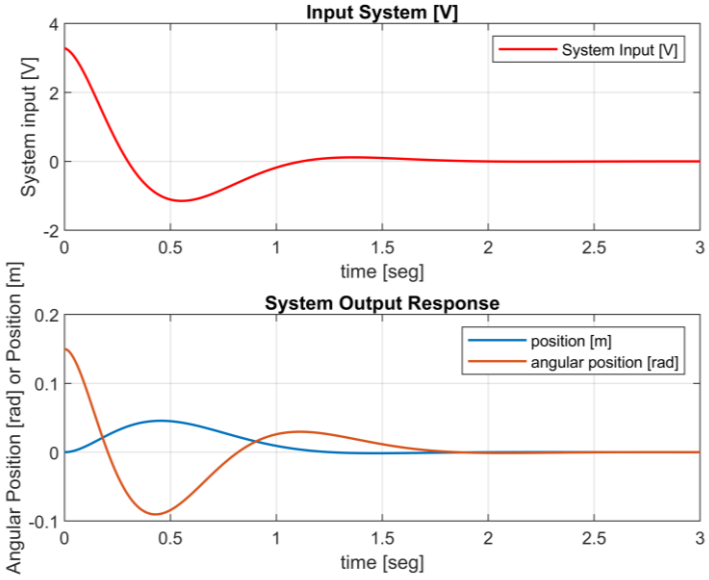

Figure 7 – The output system response.

Response for all system states can be seen in Fig. 8.

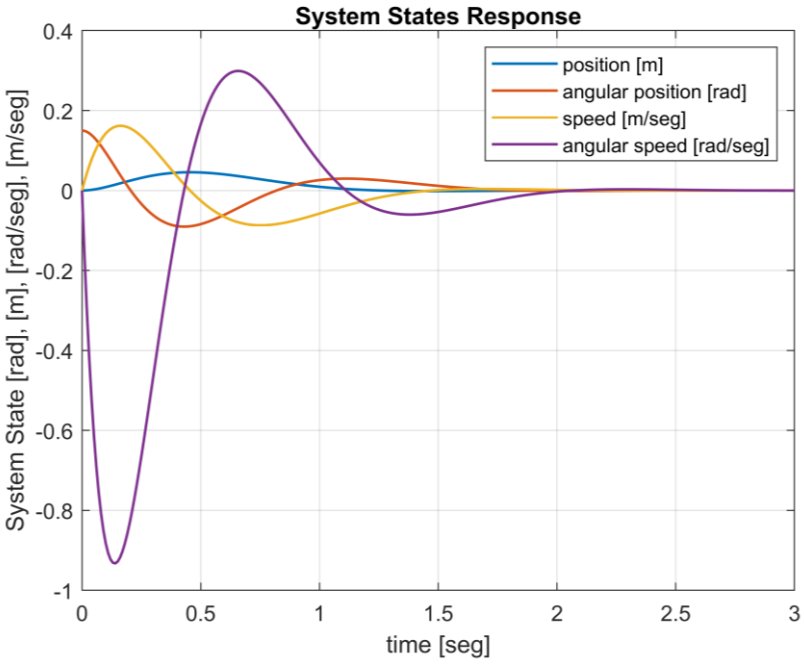

Figure 8 – System response.

The system presented settling in around 1.4 seconds as desired for both outputs. As the controller presented a good performance in the numerical simulations, it was implemented in the prototype.

HARDWARE ARCHITECTURE

Figures 9 and 10 depict the used hardware.

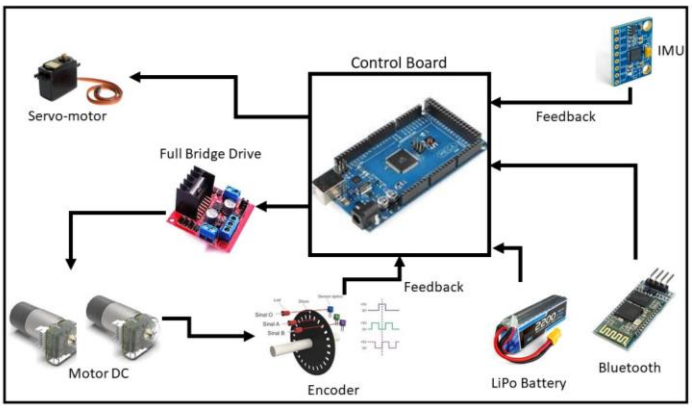

Figure 9 – Hardware architecture of the Standing Self-Balancing Wheelchair

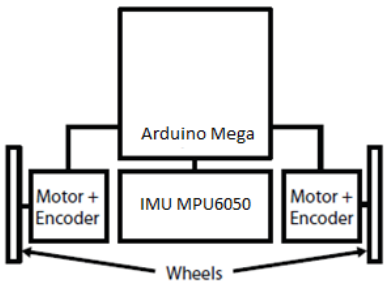

Figure 10 – Hardware architecture of the Standing Self-Balancing Wheelchair

In the full-size system, the user controls the movement with a joystick attached to the wheelchair armrest. As a small-scale prototype was built, a cell phone application was developed to control the system using a Bluetooth module. This application was made using *AppInventor* software. A polymer lithium battery was used to power the device. This battery provides 11.1 V and 220 mA.h. For the processing of the entire application, an Arduino Mega was used, which has all the necessary resources.

To control the wheelchair in the vertical position, it is necessary to measure the states of the system, in which encoders and inertial sensors were used. To drive the DC motors, it was used a full bridge driver. This driver receives a PWM signal from the control board and drives the motor proportionally to this signal. Since it is a full bridge, the driver allows the motor to be activated in both directions. To make it possible to switch between the sitting and standing positions a servomotor was employed.

The measurement of the angular position of the wheelchair was obtained from an inertial measurement unit (IMU) MPU6050. The IMU has a digital motion processor (DMP), which also provides the angular position (Iven Sense, 2013). From the point of view of computational effort, the use of DMP is interesting. It saves microcontroller processing time as there is no need for calculations to get the angular position estimate. The disadvantage of DMP is that there is no access to the calculations performed to obtain the angular position estimate. As there is an intention to use the DMP to simplify the development of the project, it was necessary to validate the measurement provided by the DMP.

Validation of the IMU Measurement

For the measurement validation process provided by the DMP, a device consisting of two columns, an axis, and a rod fixed to the axis was built. The axis has a precision potentiometer measuring the angular position of the rod. The IMU, configured to use the DMP, is also attached to the rod in other to perform the same measurement. In this way, the angular measurement of the potentiometer was used as a standard to compare with the measurement of the IMU. An angle protractor was used to calibrate the measurement provided by the precision potentiometer. The device built for the validation process can be seen in Fig. 11.

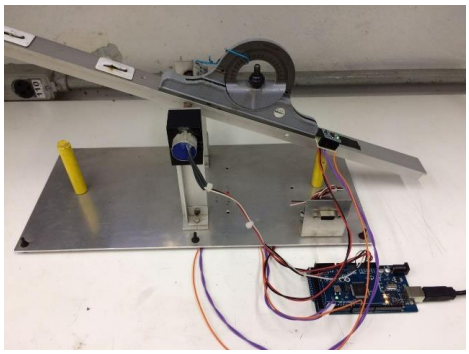

Figure 11 – Device used to validate the IMU measure.

For device data acquisition, a *LabView* program was developed having serial communication with the *Arduino*. The data is processed in *Arduino* and sent to the computer. The *LabView* code only presents the results graphically and generates an *Excel* file with the recorded data.

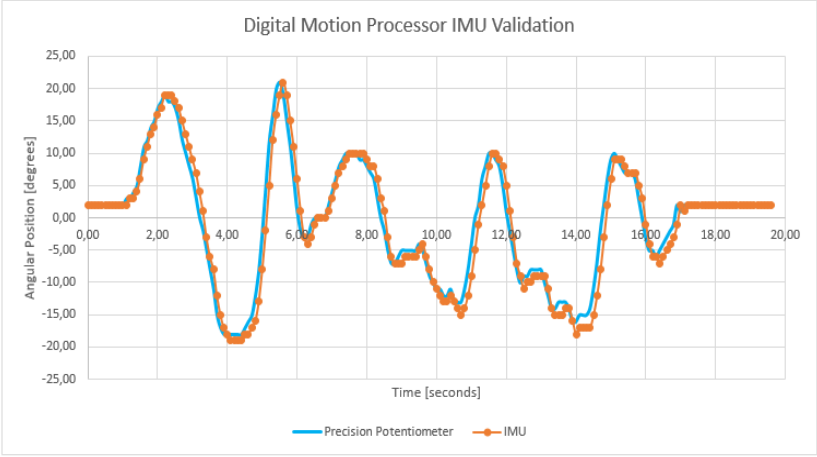

Figure 12 – Measurements realized by IMU (MPU6050)

As seen in Fig. 12, the angular position of the IMU through the DMP is very close to the standard data. This result encouraged the use of DMP.

RESULTS

After the implementation, the prototype was tested and presented very satisfactory results, being able to correct errors that caused small disturbances (small pushes) applied to the wheelchair. The results of the system in balance can be seen in Fig. 13.

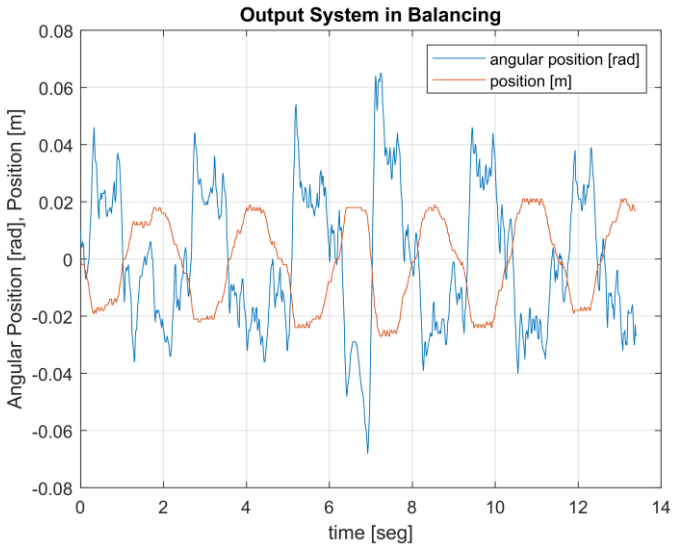

Figure 13 – Data of the prototype in balancing.

To measure the performance of the system during the development of the controller, the system was supposed to start from a condition of 0.15 rad error. The time response of the closed loop system and the amplitude of the signals were then simulated using Simulink. To compare the performance of the prototype with the results of the simulations, the prototype was tested starting from the condition of 0.15 rad of error as it was performed in the simulations. Fig. 14 shows the comparison between the simulation of the system and the result of the prototype.

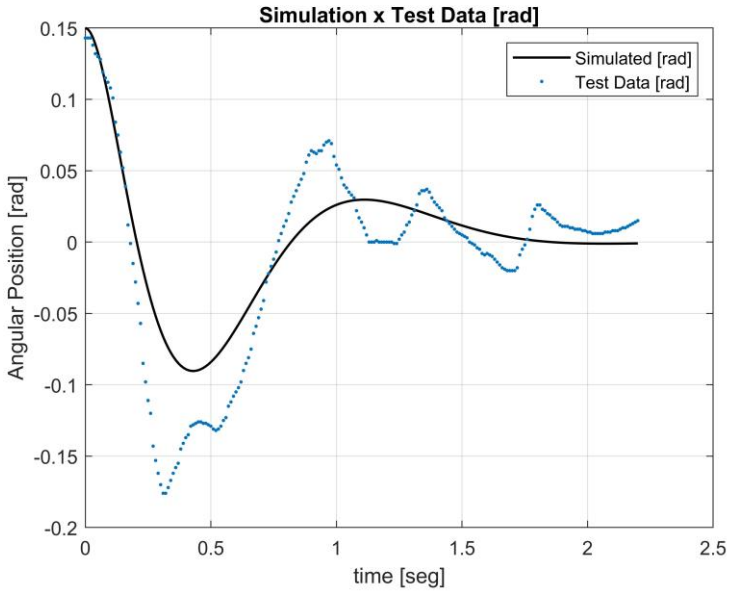

Figure 14 – Simulation and real prototype data.

As shown in the Fig. 13, there are small variations around the equilibrium position, a problem attributed to the clearance existing in the motor axis. The motors make some effort until the system overcomes the clearance, introducing a sudden movement and causing small unwanted variations. The same variations can been seen in Fig. 14, where the controller performance is tested and compared with the model simulation. Still, the results were surprisingly good.

CONCLUSION

The design of an innovative wheelchair that could operate in an upright and self-balanced position is considered in this work. To achieve the proposed goals, initially, the system was modelled and analyzed. Intrinsic system conditions such as linearity and stability were verified. The controller designed through the pole allocation approach was validated in a simulation environment using the mathematical model of the system developed by the authors. In the simulations, the system showed good performance, meeting the requirements initially established. For practical verification of the system, a small-scale prototype was built. Data from the working prototype were acquired to verify the real performance of the system. As shown, the real data of the prototype well matched the data obtained in the simulation.

It is still important to point out that initially, in the design of the controller, a settling time of 0.8 sec was adopted, resulting in high gains for the controller. When implementing the controller, the prototype showed a lot of vibration, which was attributed to the amplification of the system noise. However, the system stopped vibrating when a set time greater than 1.0 sec was used, reducing the gains of the controller.

For future works, the implementation of robust control techniques is envisaged, so that the wheelchair performance and safety are improved. Considering users with different characteristics, it is important to consider the uncertainties in the mathematical model. Also, the test of the controller for different speeds for the case when the wheelchair moves in the upright configuration are needed, to better evaluate the proposed prototype. Finally, it will be necessary to carry out an in-depth study of the wheelchairs sensor system, including devices to avoid collisions and falls that may harm users.

REFERENCES

Deng, B., Dong, J., and Chen, Y. (2021). Leg-wheel composite wheelchair based on parallelogram mechanism. Journal of Physics: Conference Series, 1865(3) doi:10.1088/1742-6596/1865/3/032002

Fahmi, A., Sulaiman, M., Siradjuddin, I., Wirawan, I. M., Jaya, A. S. M., Jiono, M., and Amalia, Z. (2020). Stabilized controller of a two wheels robot. Bulletin of Electrical Engineering and Informatics, 9(4), 1357-1363. doi:10.11591/eei.v9i4.1965

Iven Sense (2011). MPU-6000/MPU-6050 Register Map and Descriptions. Document Number: RM-MPU-6000A-00, Revision: 4.2, Pag. 46

Jameel, H. F., Mohammed, S. L. and Gharghan, S. K. (2020). Wheelchair control system based on gyroscope of wearable tool for the disabled. IOP Conference Series: Materials Science and Engineering, 745(1) doi:10.1088/1757-899X/745/1/012091

Kien, V. N., Quang, N. H. and Trung, N. K. (2021). Application of model reduction for robust control of self-balancing two-wheeled bicycle. Telkomnika, Telecommunication Computing Electronics, and Control, 19(1), 252-264. doi:10.12928/TELKOMNIKA.V19I1.16298

Kim, B. W., and Park, B. S. (2016). Robust control for the segway with unknown control coefficient and model uncertainties. Sensors (Switzerland), 16(7) doi:10.3390/s16071000

Mohammed, I. K., and Abdulla, A. I. (2020). Balancing a segway robot using an LQR controller based on genetic and bacteria foraging optimization algorithms. Telkomnika, Telecommunication Computing Electronics, and Control, 18(5), 2642-2653. doi:10.12928/TELKOMNIKA.v18i5.14717

Su, Y., Wang, T., Zhang, K., Yao, C. and Wang, Z. (2020). Adaptive nonlinear control algorithm for a self-balancing robot. IEEE Access, 8, 3751-3760. doi:10.1109/ACCESS.2019.2963110

Thai, P. Q., Tai, V. C. and Tien, L. M. (2020). Design and implementation of an electric wheelchair operating in different terrains. International Journal of Mechanical Engineering and Robotics Research, 9(6), 797-802. doi:10.18178/ijmerr.9.6.797-802